



Sequestration of Congo Red from aqueous solution using raw and citric acid-modified *Dicerocaryum eriocarpum* biomass: isotherm, kinetics and thermodynamics

Mobolaji M. Jegede¹ · Olatunde S. Durowoju¹ · Joshua N. Edokpayi¹

Received: 1 April 2023 / Accepted: 23 January 2024 / Published online: 27 February 2024
© The Author(s) 2024

Abstract

In recent times, dyes such as Congo Red have proven to be resilient environmental pollutants affecting freshwater portability among other media. Its toxicity to humans, animals and plant life is both a cause of concern and a motivation to prioritize decontamination. Many materials have been explored for the removal of this pollutant via adsorption; however, there are notable areas of improvement. *Dicerocaryum eriocarpum* (DE) seed is a non-toxic, cost-effective plant material which is possible as a sorbent and has not been reported in Congo Red sequestration. This research is therefore based on the removal of Congo Red dye from aqueous solution using raw (RDE) and citric acid-modified DE (CDE). The sorbents were characterized before and after sorption using various characterization techniques such as FTIR, EDS, SEM and BET. The effects of contact time, adsorbent dosage, concentration, pH and temperature were optimized during the experiment. According to experimental findings, modification with citric acid resulted in a reduction of the equilibration interval from 90 to 60 min. Sorption effectiveness increased with an increase in temperature for CDE but a decrease in temperature for RDE. The equilibrium data were best described by the Langmuir isotherm with maximum sorption capacity (q_{max}) of 51.02 mg/g and 53.19 mg/g for RDE and CDE, respectively. Pseudo-second-order model better suited the kinetic data, while thermodynamic analysis revealed a spontaneous sorption process. Five cycles of desorption experiments using 0.1 M NaOH revealed that the regenerated sorbent effectively removed CR dye for the first three cycles at comparable efficiency to the virgin samples. This study therefore supports the use of DE seed as an easily accessible and efficient sorbent for remediation of harmful dyes from water.

Keywords *Dicerocaryum eriocarpum* seeds · Citric acid · Congo Red · Dyes decontamination · Sorption process

Introduction

The contamination of freshwater resources by anthropogenic activities has continued to increase globally despite several environmental awareness and campaigns. Stringent guideline values have been adopted by several countries due to the impact of environmental contaminants. A notable group of chemicals that have a great impact on freshwater systems and the aquatic biota are dyes.

There is a growing demand for more colored products in the textile and leather industries due to the aesthetic value they add to various products. Most dyes are highly resistant to the action of alkalis, acids and water, thus highlighting their environmental persistence as well as resistance to degradation (Harja et al. 2020; Manzoor et al. 2022). Unlike metal and non-metal contamination, a little amount of dye can significantly affect the aesthetic quality of water, thus increasing the biochemical and chemical oxygen demands of those water bodies. They have the capacity to affect photosynthesis and inhibit plant growth (Berradi et al. 2019; Jeyavishnu and Alagesan 2020). Dyes have bio-accumulative tendencies and can enter the food chain causing several disease burdens both to plants and animals.

There are natural and synthetic dyes. Natural dyes are often derived from plants and animals, but because of high demand, dyes are made commercially via synthesis from

✉ Joshua N. Edokpayi
Joshua.Edokpayi@univen.ac.za

¹ Water and Environmental Management Research Group, Faculty of Science, Engineering and Agriculture, University of Venda, South Africa, Private Bag X5050, Thohoyandou 0950, South Africa

precursor elements (from minerals). Dyes are often used in the textile, pulp and paper industries, photographic, ink, food and cosmetic industries as well as the plastic and leather industries (Edokpayi et al. 2020; Jegede et al. 2021). A common example of a synthetic dye is Congo Red (CR), which is an azo dye and is utilized extensively in the industry due to its exceptional efficiency. There is, however, a serious concern about the damaging impact it has on the environment (Sarkar et al. 2017; Edokpayi et al. 2019; Manzoor et al. 2022). Studies have revealed that CR can degrade into aromatic amines, a class of substance that is very toxic to the environment and has carcinogenic and mutagenic effects on humans (Sarkar et al. 2017; Harja et al. 2020).

Several techniques such as physical, chemical and biological techniques have been used for the decontamination of dyes from environmental media with varying degree of success (Mohebbali et al. 2019; Javid et al. 2020). The success of these techniques frequently depends on the type of dye contained in wastewater; therefore, their specific use may be constrained (Zaharia and Suteu 2009; Singh et al. 2020). Further constraints of these techniques include the high budget and poor regeneration potential (Farias et al. 2017; Edokpayi and Makete 2021).

Sorption techniques using agricultural waste have been explored as a low-cost, environmentally abundant and friendly means of sequestering hazardous dyes from various environmental media. Their physical and chemical traits including functional charges of their cellulose, hemicellulose and lignin contents favor their ability to effectively bind a variety of contaminants, including dyes (Yagub et al. 2014; Edokpayi and Makete 2021). Modification of the plant biomass has been reported to achieve improved dyes sequestration at shorter time (Jegede et al. 2021). Among them include coffee waste for the removal of Reactive Black 5 and Congo Red (Wong et al. 2020), pine tree leaf biomass for the removal of Methylene Blue (Sen 2023), and anchote peel for the removal of methyl orange (Hambisa et al. 2023).

Dicerocaryum Eriocarpum (DE) is a constantly available flora with a pointed stud which is commonly found in grassland fields (Mannzhi and Edokpayi 2023). On exposure to water, the plant parts such as leaves, flowers and stem become slimy and parts of the plant have been used for medicinal purposes in Vhembe District, South Africa (Odiyo et al. 2017). To the best of the authors' knowledge, *Dicerocaryum Eriocarpum* seed has not been researched for the removal dye despite qualifying as an affordable and ecofriendly material.

In this study, we report the use of (DE) seeds as an sorbent to remove toxic dye from aqueous solutions. The effect of modification of DE using citric acid (CA) on the sorption process is also reported. Furthermore, the influence of change in water chemistry and application of both sorbents on a wide variety of dyes is also reported.

Materials and methods

Sample collection, preparation and modification

DE plants were collected from villages around the University of Venda, Limpopo Province, South Africa. The seeds were manually sorted, washed in distilled water to eliminate clinging contaminants and dried for 72 h at 50 °C in the oven. The dried seeds (RDE) were ground in a Retsch RS 200 pulverizer and sieved in a King-test VB 200/300 sieve shaker.

The procedure for the modification of RDE followed closely those reported by Yan et al. (2018) and Zhang et al. (2019). Ten grams of RDE was added to 100 mL of 0.5 M CA in a 250-mL shaking container. For 90 min, the mixture was agitated in a water bath at 250 rpm. The mixture was then put into a stainless steel pan and dried for 24 h at 50 °C in an oven. Following that, the oven's temperature was increased to 120 °C for 90 min to facilitate a thermochemical interaction between the acid and the RDE. To eliminate excess CA, the dry material was soaked in distilled water and repeatedly washed until no turbidity was visibly observed as confirmation that the excess CA had been removed. The resulting material was dried for 48 h in an oven at 50 °C and was then left to cool, after which it was crushed and stored in an airtight container. The modified DE powder was labeled CDE.

Preparation dye solution

The CR dye (analytical grade) was acquired from Fisher Scientific, USA. In 1000-mL volumetric flask, 1 g of CR dye was dissolved in deionized water to make a dye stock solution. A known concentration of the stock solution was diluted with the right volume of deionized water to make various working test solutions of the desired concentrations. The wavelength of maximum absorption was determined to be 496 nm using a UV–Vis Spectrophotometer.

Characterization of the adsorbent

The functional groups responsible for the characteristics of the sorbents before and after sorption were examined using a PerkinElmer 100 FTIR spectrophotometer (Waltham, MA, USA). To collect bands relevant to the sample, the spectroscopic spectra were scanned over the wavelength range of 4000–500 cm^{-1} (Ologundudu et al. 2016).

An energy-dispersive X-ray spectrometer (EDS) instrument in conjunction with a scanning electron microscope (SEM) (TESCAN, VEGA 3 SBU, Brno, Czech Republic) was used to analyze the surface morphology and elemental

composition of sorbents before and after CR dye sorption adhering to the method described by Edokpayi et al. (2015). Using a Tristar II Micromeritics (USA) analyzer, the Brunauer, Emmet and Teller (BET) Technique was used to analyze the texture of the powdered sorbent. Samples were degassed overnight at 50 °C in a vacuum (Brunauer et al. 1938). Using nitrogen gas at 77 K, the surface area, total pore volume and average pore diameter were determined. With the help of a t-plot and the Barrett–Joyner–Halenda (BJH) model (Barrett et al. 1951), the distribution of pore size and pore volume was estimated (Lippens and De Boer 1965).

Determination of point of zero charge (PZC)

The point of zero charge indicates the pH where the sorbent surface is neutral. To perform this test, 40 mL of 0.01 M NaCl solution (99.5%) was placed into seven bottles and the initial pH (pH_o) was determined using a pH meter. The pH_o values were adjusted to pH in the range of 2–10 in all the containers with 0.1 M HCl (37%) and 0.1 M NaOH (99%) solution, respectively. Each bottle received 0.15 g of sorbent, which was added before being shaken in a water bath at 30 °C for 24 h. The PZC was computed by plotting changes in pH values versus the initial pH value. The point of intersection on the x-axis where pH_f = pH_o is known as the PZC of the sorbent.

Sorption studies

Batch equilibrium experiments were performed in this study. For each sorption test, 0.05, 0.10 and 0.15 g masses of the sorbent were each added to 40 mL of CR dye solution (40 mg/L) in a 100-mL shaking bottles. The sample was shaken in an Ecobath Labotech water bath shaker at a temperature of 30 °C and an agitation speed of 200 rpm. The samples were taken out of the shaker at various intervals and centrifuged for 10 min at 2800 rpm. A UV–visible spectrophotometer operating at a wavelength of 496 nm was used to estimate the final concentration of the supernatant. The effects of experimental variables such as contact time (5–180 min), sorbent dosage (0.5–5.0 g/L), sorbate concentration (40, 60, 80 mg/L), temperature (30–80 °C) and pH (2–10) on the sorption were examined. The experiments were conducted in triplicate.

To test the effects of change in water chemistry, surface water drawn from the Mutale River in South Africa was used. Here, the effectiveness of removing CR dye was compared to an experiment using deionized water. To evaluate how well the sorbents work with different kinds of dyes, other dyes such as Rhodamine B, Methylene blue, Methylene orange, Crystal Violet and Malachite green were also tested to determine the removal effectiveness.

After every batch experiment, the amount of sorption q_e (mg/g) was calculated using Eq. (1) (Edokpayi and Makete 2021):

$$\text{Quantity sorbed (mg/g)} = \frac{(C_o - C_e)}{m} \times V \quad (1)$$

where C_o (mg/L) is the initial concentration of the dye, C_e (mg/L) is the equilibrium liquid phase concentration of the sorbate, V (L) is the volume of the solution and m (g) is the mass of sorbent.

The percentage removal of the dye was computed using the relation in Eq. (2):

$$\text{Percentage removal} = \frac{(C_o - C_f)}{C_o} \times 100 \quad (2)$$

where C_o and C_f (mg/L) are the initial and final concentrations of the dye solution.

Adsorption kinetics

Kinetic models such as the pseudo-first-order, pseudo-second-order and intra-particle diffusion models were used to investigate the mechanism and rate at which CR is sorbed onto the sorbents. The linear forms of the kinetic models (Eqs. 3 and 4) were used in this study (Lagergren 1898; Ho and McKay 1998):

$$\log (q_e - q_t) = \log q_e - \left(\frac{k_1 t}{2.303} \right) \quad (3)$$

$$\frac{t}{q_t} = \frac{1}{k_2 q_e^2} + \frac{t}{q_e} \quad (4)$$

where k_1 and k_2 are the rate constants of the pseudo-first- and pseudo-second-order models. q_e and q_t are the amounts of CR sorbed at equilibrium and at a specific time t , respectively.

The linear expression of the intra-particle diffusion model is given by Eq. (5):

$$q_t = k_p t^{0.5} + C \quad (5)$$

where k_p is the intra-particle diffusion rate constant (mg/g min), C is the intercept (mg/L) and q_t is the amount of dye sorbed (mg/g) at time t (min) (Webber and Morris 1963).

Additionally, this model is utilized to handle experimental data that were obtained by the plot of q_e against $t^{0.5}$. The graph's slope and intercept was used to calculate the values of K_p and C . It is presumed that internal diffusion is the only rate-limiting phase in the reaction if the plot intercepts at the origin (Lin et al. 2020). The intercept provides information about the boundary layer's thickness. The thickness increases with increasing C

values (Corda and Kini 2018). The intra-particle rate constant is the computed value of the slope of the linear plot.

Adsorption isotherms

The linearized forms of the Langmuir, Freundlich and Temkin adsorption isotherm models were used to examine the equilibrium data obtained. The linear form of the Langmuir model is presented in Eq. 6

$$\frac{1}{q_e} = \frac{1}{q_{\max}} + \left(\frac{1}{K_L q_{\max}} \right) \frac{1}{C_e} \quad (6)$$

where q_{\max} is the amount of dye sorbed to the highest possible level (in mg/g) and K_L is the Langmuir constant (in L/mg) (Langmuir 1916). q_e and C_e were as described in Eq. 4. The q_{\max} and K_L were determined from the intercept and slope of the plot, respectively. Equation (7) was used to assess the sorption process' adherence to the Langmuir model:

$$R_L = \frac{1}{(1 + K_L C_o)} \quad (7)$$

where K_L is the Langmuir constant (in L/mg). $R_L > 1$ denotes an unfavorable situation, $R_L = 1$ denotes a linear situation, $0 < R_L < 1$ denotes a favorable situation, and $R_L = 0$ denotes an irreversible monolayer sorption process (Edokpayi et al. 2015; Inyinbor et al. 2015).

Equation (8) expresses the Freundlich isotherm model, which explains a multi-site adsorption for heterogeneous surfaces (Freundlich, 1906).

$$\log q_e = \log K_F + \log C_e \quad (8)$$

where K_F is the sorption capacity (L/mg), $\frac{1}{n}$ refers to the sorption intensity, q_e and C_e are as described in Eq. 4. From a linear plot of $\log q_e$ against $\log C_e$, the slope and intercept of the graph can be used to deduce the constants n and K_F . A favorable sorption process is also indicated by the value of $n > 1$.

Temkin isotherm assumes that the heat of sorption of dye molecules on the surface of the sorbent decreases linearly rather than logarithmically as stated by Freundlich's formula (Temkin and Pyzhev 1940). Equation (9) represents the Temkin model in linear form.

$$q_e = B_1 \ln K_T + B_1 \ln C_e \quad (9)$$

B_1 is the Temkin constant; K_T represents the equilibrium binding constant (Lm g⁻¹) and is determinable from the slope and intercept of q_e vs. $\ln C_e$.

Thermodynamics of sorption

The change in both enthalpy (ΔH) and entropy (ΔS) of the sorption process was examined using the Van't Hoff plot (Eq. 10) (Van't Hoff 1884). The enthalpy and entropy were determined from the slope and intercept derived from the plot of $\ln K_o$ vs $1/T$.

$$\ln K_o = \frac{\Delta S^\circ}{R} - \frac{\Delta H^\circ}{RT} \quad (10)$$

where K_o is the equilibrium constant, R the gas constant while T is the temperature.

The feasibility and spontaneity of the process were computed using Eq. 11.

$$\Delta G^\circ = -RT \ln K_o \quad (11)$$

where ΔG° is the changed in Gibb's free energy.

Desorption study/regeneration

Desorption research is crucial, especially when re-using a sorbent, and the environmentally acceptable disposal means of a used sorbent is dependent on certain factors. This results in practical, cost-effective, wastewater treatment which helps to avoid sludge build-up and reduces environmental contamination. Desorption was carried out based on the procedure described in Edokpayi et al. (2015). 0.15 g of sorbent was added to three 100-mL shaker bottles that contained 40 mg/L CR solution as part of a desorption experiment. These were shaken for 90 min at 200 rpm in an eco-bath shaker with the temperature set at 30 °C. After the allotted time had passed, the expended sorbents were retrieved and thoroughly cleaned with distilled water to remove any remaining color. Deionized water, 0.1 M HCl (37%) and 0.1 M NaOH (99%) were used as possible desorbing agent. Each 100-mL shaker bottle containing the used sorbent received 40 mL of the desorbing agents, which were then mixed for 90 min at a speed of 200 rpm at 30 °C. Following centrifugation, the supernatant was examined to ascertain the final concentration of the solution following desorption. Equation 12 was used to compute the percentage desorption.

$$\text{Desorption \%} = \frac{\text{Desorbed dye concentration}}{\text{Initial adsorbed dye concentration}} \times 100 \quad (12)$$

Results and discussion

1: Sorbents characterization

Fourier transform infrared spectroscopy (FTIR)

In the modified sorbent (CDE), a broad peak was recorded at 3325 cm^{-1} which corresponds to the presence of O–H stretch of the alcohol group (Fig. 1). A similar peak at 3323 cm^{-1} was also recorded for the RDE as noticed by Mannzhi and Edokpayi (2023). CH-stretch of aliphatic group was recorded for both sorbents around $2845\text{--}2913\text{ cm}^{-1}$ and $2841\text{--}2937\text{ cm}^{-1}$, respectively (Wong et al. 2020). The peak recorded at 1019 cm^{-1} (RDE) and 1026 cm^{-1} (CDE) can be attributed to C–O stretch of the carboxylate groups. CDE spectra evidently did not differ significantly from raw RDE except for a shift in peak to higher absorbance levels and the emergence of new peaks at 2913 and 2845 cm^{-1} assigned to C–H stretch of alkane/aliphatic group, as well as 1621 and 1589 cm^{-1} assigned to C=C stretch of ester and carboxylate groups, respectively (Ren et al. 2018).

The spectra of the spent raw and modified DE biosorbents (SRDE and SCDE) are displayed in Fig. 2A, B. Changes were observed in them after sorption when compared to RDE and CDE. SRDE and RDE showed similar spectra line patterns, although there was movement of peaks/band to higher absorbance values and the peaks at 2158 and 2027 cm^{-1} became more pronounced. SCDE

spectra showed diminishing peaks at 2913 and 2845 cm^{-1} . The decrease in band intensities as well as appearance and disappearance of peaks suggests that some of the functional groups were utilized for dye adsorption (Inyinbor et al. 2015).

Scanning electron micrograph (SEM)

Figure 3 displays the SEM micrographs of the sorbents before and after sorption. The micrograph of CDE show a larger surface area with a flasky structural surface when compared to RDE. This could be due to the modification. Also, the surface of CDE showed improvement in sharpness (Ren et al. 2018; Oyekanmi et al. 2019). Due to the sorption of the CR dye molecule onto the active surfaces of the sorbent, the SEM after sorption (SRDE and SCDE) shows a more distinct and occupied morphology with flaky protuberances.

Energy-dispersive X-ray spectroscopy (EDS)

Figure 4 shows the EDS spectra obtained before sorption, and the quantitative results of their elemental compositions are also presented in Table 1. Oxygen and carbon were among the important components found in EDS spectra along with other elements that make up a little amount. For RDE, the atom percentage values of 28.44% (O) and 64.64% (C) were reported, but for CDE, the values were 17.16% (O) and 76.21% (C). The observed rise in carbon atom percentage and reduction in oxygen atom percentage in CDE as

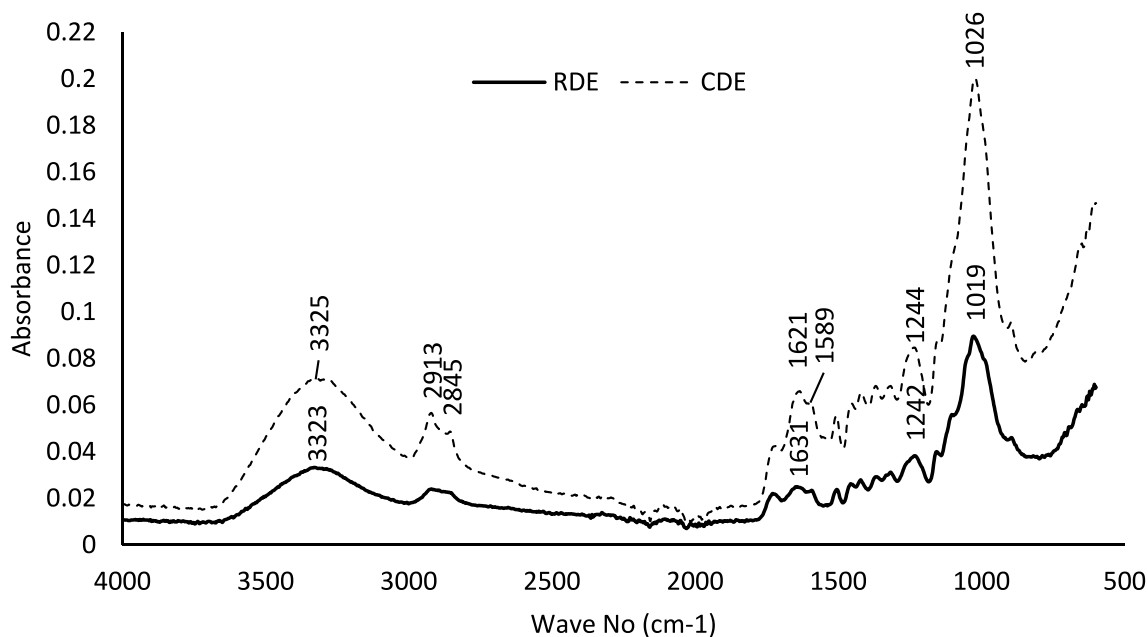


Fig. 1 FTIR spectra of RDE and CDE before sorption

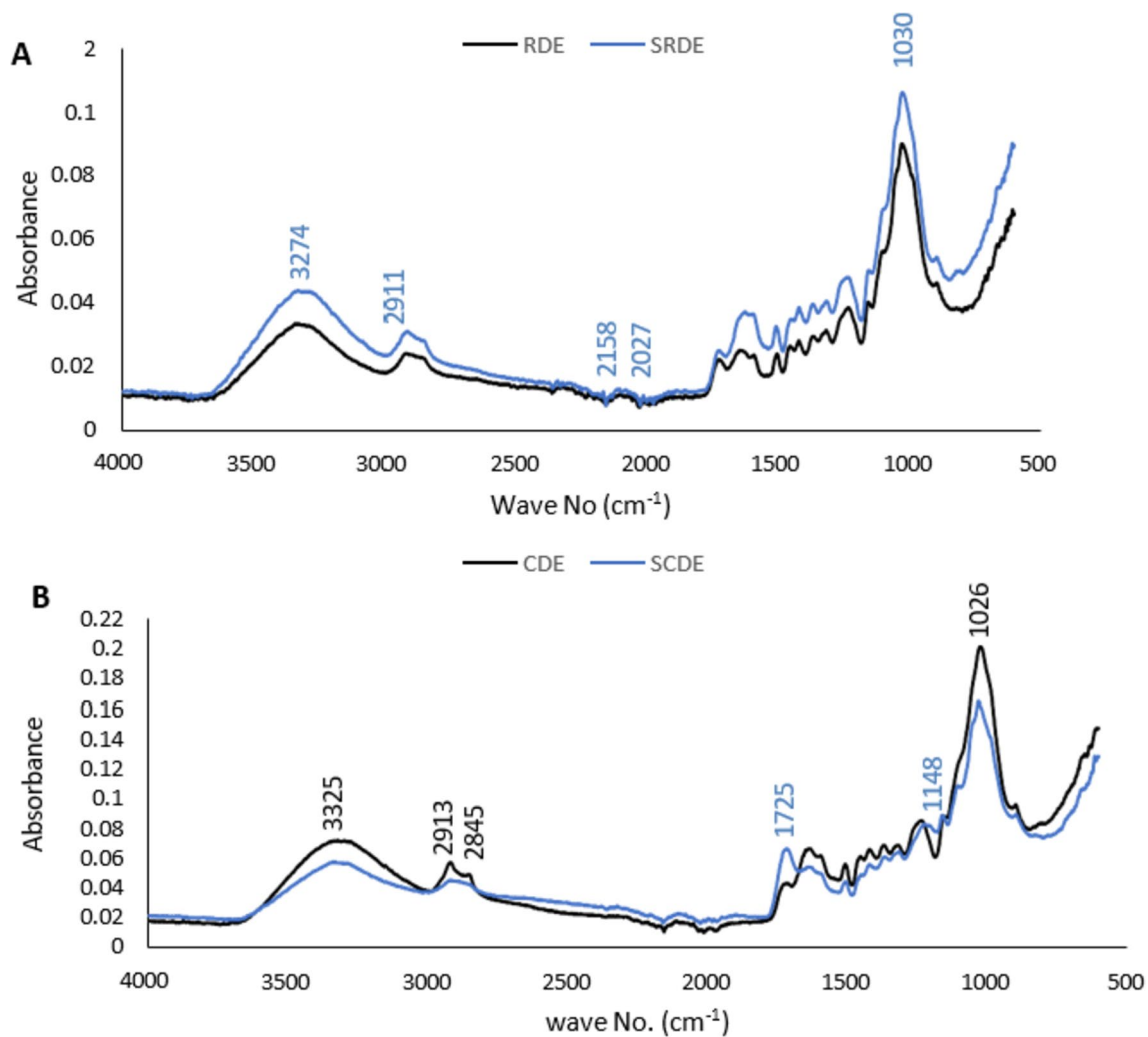


Fig. 2 FTIR spectra of **A** RDE and SRDE, **B** CDE and SCDE

compared to RDE may be the result of the chemical alteration (Olakunle et al. 2017).

Ojo et al. (2017) reported that due to bond breaking and connections caused by chemical alteration of sorbents at high temperatures, the volatile contents of the sorbents became unstable, increasing the percentage of active carbon. Bello et al. (2013) correctly noted that the performance of the sorbent for the sorption process improved with increasing carbon content. As a result, CDE is probably more effective at removing dye than RDE. After sorption, the percentage of carbon and oxygen atom of the sorbents significantly changed which implies that sorption has occurred.

The Brunauer–Emmett–Teller method (BET)

The BET surface area of the modified sorbent (0.97 m²/g) was slightly higher than the raw sorbent (0.78 m²/g) (Table 1). Both sorbents are not microporous, and CDE

is more likely to have increased sorption due to its slight increase in surface area over RDE. Low surface area values have also been observed in some earlier studies on dye sorption from aqueous solution employing plant-based sorbents (Inyinbor et al. 2015; Sharma and Tiwari 2016; Lin et al. 2020). Because certain polar functional groups on the surfaces of the sorbent were removed by acidic washing of the cell wall, there was a slight increase in surface area after acid alteration (Inyinbor et al. 2015).

Figure 5 shows the adsorption/desorption plot for RDE and CDE, respectively. At high relative pressure beyond 8 (p/p^0), both show a sharp rise in quantity adsorbed and the isotherms were almost overlapped for both sorbents which indicates the presence of identical adsorption.

Based on IUPAC classification, the isotherms were most relatable to the type II isotherm which depicts unrestricted monolayer–multilayer adsorption (Sing et al. 1985). However, the desorption isotherms drifted

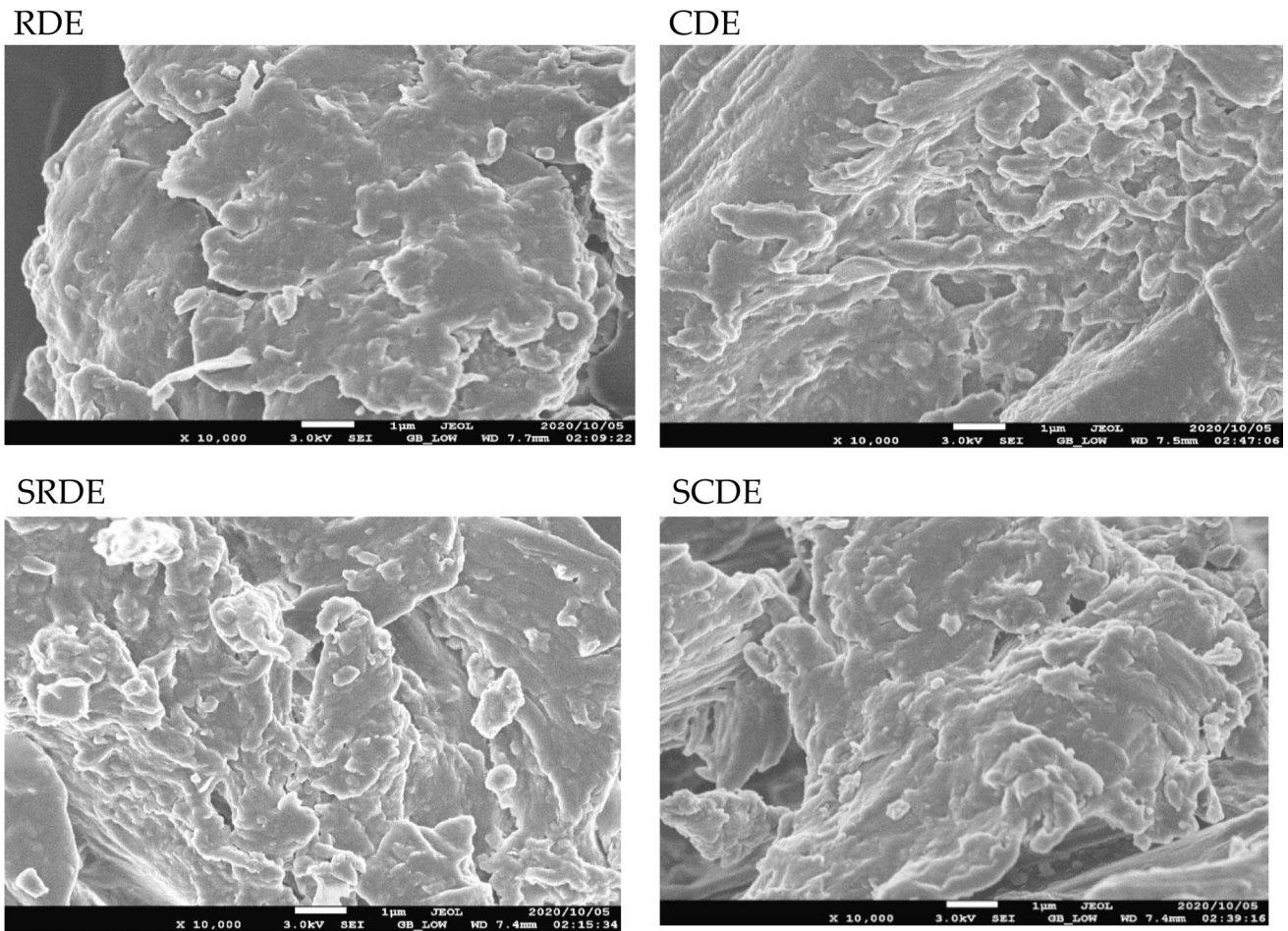


Fig. 3 SEM of RDE and CDE before and after CR dye sorption (×10,000)

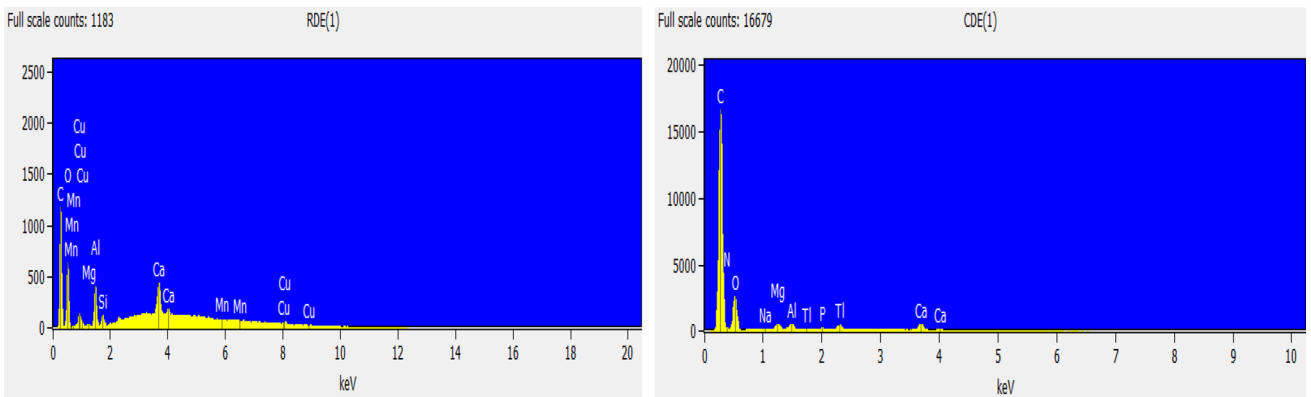


Fig. 4 EDX spectra of RDE and CDE before CR sorption

Table 1 Elemental composition of sorbents and BET structure parameters of sorbents

Sorbents	% of C Atom	% of O Atom	BET surface area (m ² /g)	Total pore volume (cm ³ /g) × 10 ⁻⁴	Average pore diameter (Å ^o)
RDE	64.64	28.44	0.78	0.21	371
CDE	76.21	17.16	0.97	1.38	363

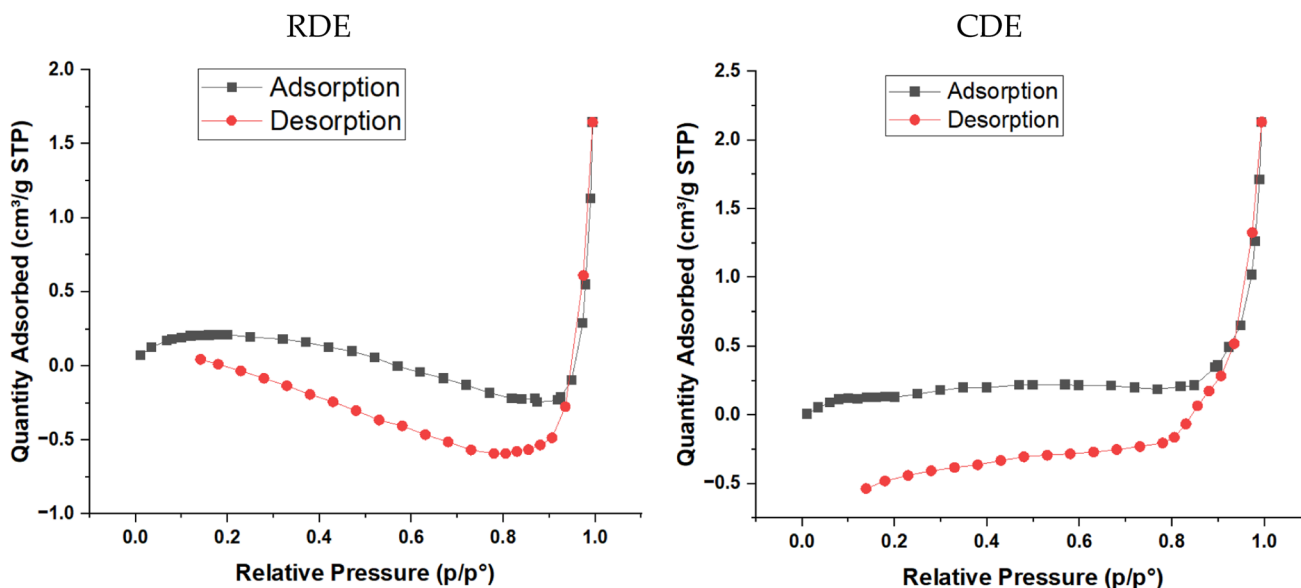


Fig. 5 N₂ adsorption/desorption isotherm for RDE and CDE

from the expected isotherm to form a hysteresis (Kong et al. 2019). The occurrence of the hysteresis further reinforces the monolayer–multilayer adsorption as well as the involvement of ranging pore sizes on the sorbent surfaces as reported by Bwatanglang et al. (2023).

Point of zero charge (PZC)

Varying PZC was recorded for both sorbents (Fig. 6). RDE and CDE recorded a PZC of 6.2 and 2.8 respectively. If pH < PZC, then the surface of the sorbent will tend to attract anions as it will be positive and vice versa. Since the sorbents PZC values are in the acidic range, they would have the tendency to attract anions via electrostatic attraction (Bello et al. 2020).

Effects of experimental variables on the sorption of CR dye

Time

Figure 7 clearly demonstrates that as contact time increased, the removal effectiveness of CR dye by 0.05 g, 0.1 g and 0.15 g of the sorbents rose quickly. It is significant to note that compared to RDE, which took 90 min to reach equilibrium, CDE did so in 60 min. All the sorbent masses had a consistent tendency toward equilibrium and once equilibrium had been reached, there was no further consistent rise in CR dye removal. CDE also recorded higher removal efficiencies when compared to RDE. This implies that a sorption process involving CDE would need less sorbent for optimum dye removal. CDE's application is cost-effective compared with RDE due to its shorter equilibrium time and low dosage.

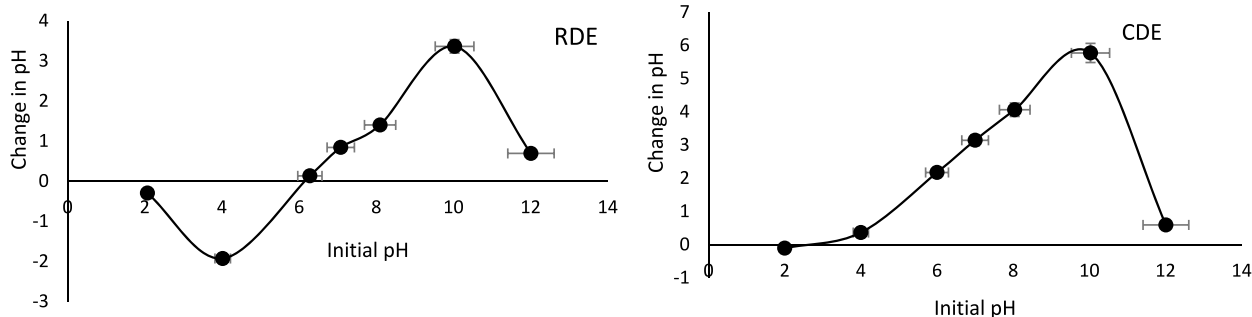


Fig. 6 PZC for RDE and CDE

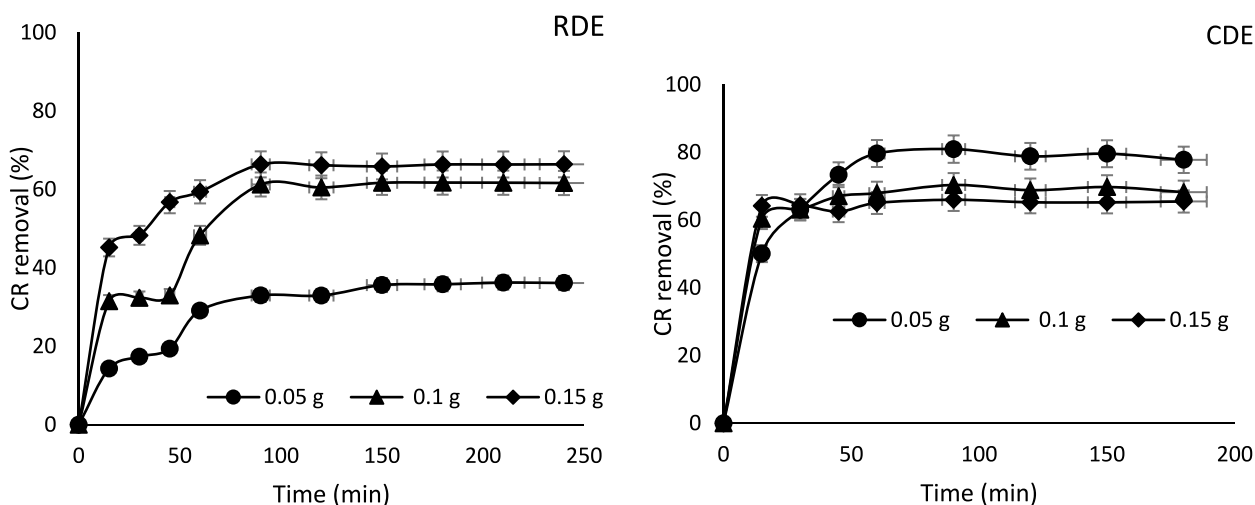


Fig. 7 Effect of time on sorption of CR dye onto RDE and CDE

The rapid removal efficiency of CR from the solution may be caused by the presence of virgin active sites on the surface of sorbents. Additionally, because a larger mass of adsorbent supplied more open active sites, the removal percentage rose with increased sorbent masses from 0.05 to 0.15 g until the surface of the sorbent was saturated leading to non-significant uptake of CR molecules (Toor et al. 2010; Tarmizi et al. 2017). In other studies based on the adsorptive removal of anionic dyes, similar patterns were reported (Felista et al. 2020; Edokpayi and Makete 2021).

Temperature

By raising the operating temperature in the range of 30 and 80 °C, the impact of temperature was examined. The results as shown in Fig. 8 indicate that an exothermic sorption process occurred because an increase in temperature did not favor the sorption of CR dye onto RDE. On the other hand,

CDE demonstrated greater CR dye removal effectiveness as temperature increased, indicating an endothermic sorption process. The increased mobility of the dye molecule and greater activation of the sorbent's active sites may be responsible for the increased uptake of CR dye by CDE at high temperatures. This result indicates that only a small amount of CDE is needed for the best CR dye removal, as the lowest mass of 0.05 g of CDE demonstrated good removal effectiveness.

Dosage and concentration

Increase in sorbent dosage led to a sequential increase in the sorption efficiency, which is expected because more vacant sites were present on the surface of the sorbents. As the sorbate dosage increases and equilibrium is eventually achieved, no further increase or decrease is recorded (Edokpayi et al. 2019). Equilibrium in this study was achieved at 4 g/L for

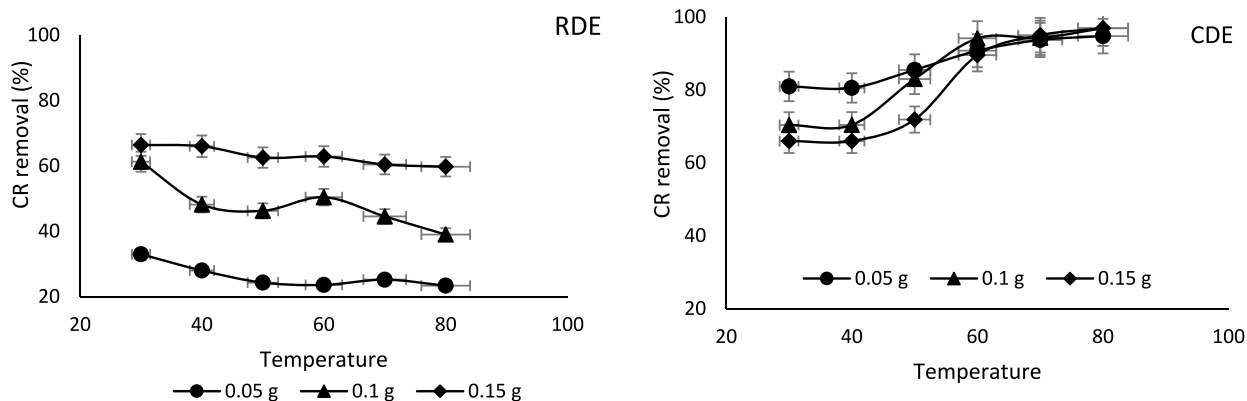


Fig. 8 Effect of temperature on sorption of CR dye onto RDE and CDE

RDE while a smaller dosage (1.5 g/L) attained comparable removal efficiency (Fig. 9). Therefore, the modification of the sorbent aided the removal efficiency recorded at lower dosage. Regardless of the different sorbent dosages, identical removal efficiencies of CR were observed at equilibrium. This result is also in line with the idea that a low dosage of CDE is necessary for maximum effectiveness and thus less production of sludge.

pH

pH is a very important experimental driver in sorption processes as some sorption processes can be aided or retarded by a change in pH value. Maximum sorption efficiency was recorded at a pH value of 2 for both sorbents (Fig. 10). This finding agrees with that of the PZC showing the potential of increased sorption in the acidic pH range. Thus, at lower pH the surface of the sorbent is positive and capable of attracting CR which is an anionic dye chiefly via electrostatic

interaction. Therefore, at increased pH value the surface becomes negative, leading to a decrease in sorption capacity due to electrostatic repulsion between the negatively charged sorbent surface and the anionic dye (Olakunle et al. 2017; Zhou et al. 2018).

Change in water chemistry

By comparing the removal efficiencies of experiments done with simulated CR dye wastewater created with surface water and that of deionized water, the effect of changes in water chemistry on the sorption of CR dye from aqueous solution was studied. The experiment's findings, as graphically displayed in Fig. 11, show that surface water exhibits more CR dye sorption than deionized water. The catalytic influence of surface water ions on the sorption process may be the cause of surface water's higher removal efficiency (Edokpayi et al. 2019). These ions have the tendency to hasten the uptake of CR dye from an aqueous solution onto

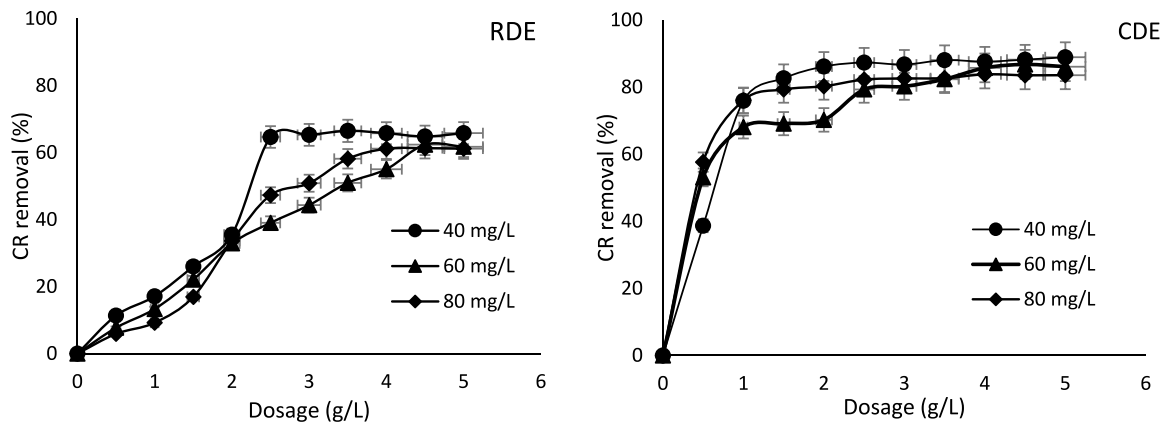


Fig. 9 Effect of dosage and concentration on sorption CR dye onto RDE and CDE

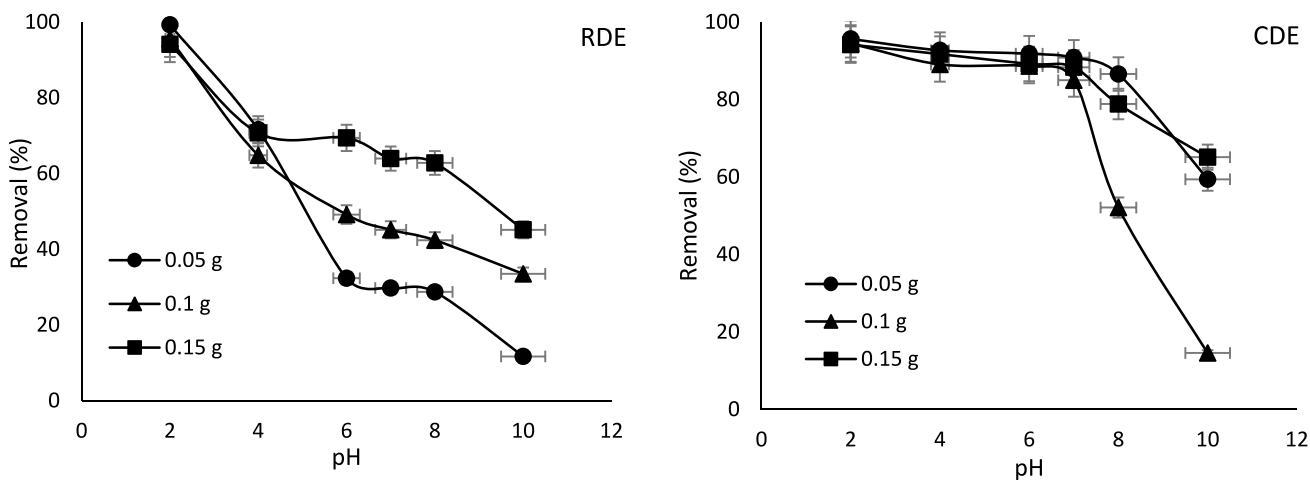


Fig. 10 Effect of pH on the uptake of CR dye onto RDE and CDE

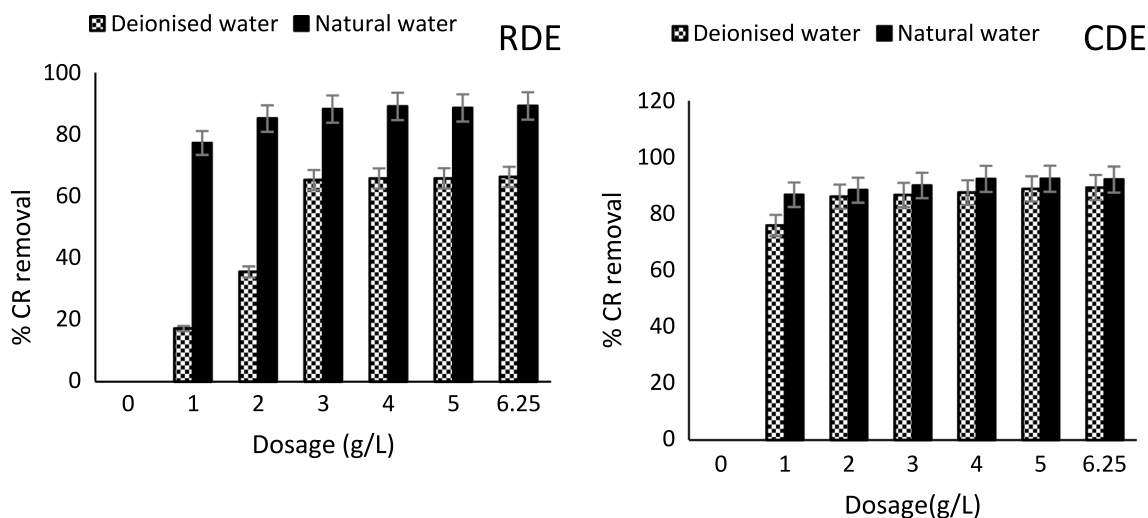


Fig. 11 Effect of change in water chemistry on the sorption of CR dye onto RDE and CDE

the sorbent's active sites. This upward trend in removal efficiency in surface water is consistent with the adsorption of dyes onto some plant-based sorbents (Edokpayi et al. 2019; Jegede et al. 2021). This confirms that the sorption procedure using the new sorbent can sequester dye from actual wastewater as opposed to only simulated dye wastewater created in the laboratory.

Sorbent removal efficiency of other dyes

The ability of the sorbent to remove various other dyes from aqueous solution as effectively as CR (anionic) dye was examined. Five additional dyes were chosen, including cationic dyes like Rhodamine B, Methylene blue and Malachite green, as well as anionic dyes like Methyl orange and Erythrosine B. The graphs shown in Fig. 12 suggest that the sorbents are useful at removing the additional test dyes. The cationic-based dyes, however, reported greater removal

percentages. This result demonstrates that these innovative sorbents are useful for the efficient sequestration of other dyes. Optimal removal of other dyes by RDE was at 90 min and mass of 0.15 g, but CDE maintained optimal removal at 60 min and 0.05 g. The improved sorbent is therefore useful for industrial applications that require cost-effectiveness.

Sorption kinetics

Based on the linearized coefficient (Table 2), the pseudo-second-order kinetics is the best fit model for the sorption process as shown in Figs. 13 and 14. Similar result has been reported on the sorption of CR on various sorbent (Khan et al. 2015; Zhou et al. 2018; Zhang et al. 2019; Lafi et al. 2019; Felista et al. 2020; Wekoye et al. 2020).

To further understand the mechanism and rate-controlling processes affecting the sorption kinetics, the Webber–Morris intra-particle diffusion model was utilized. This model

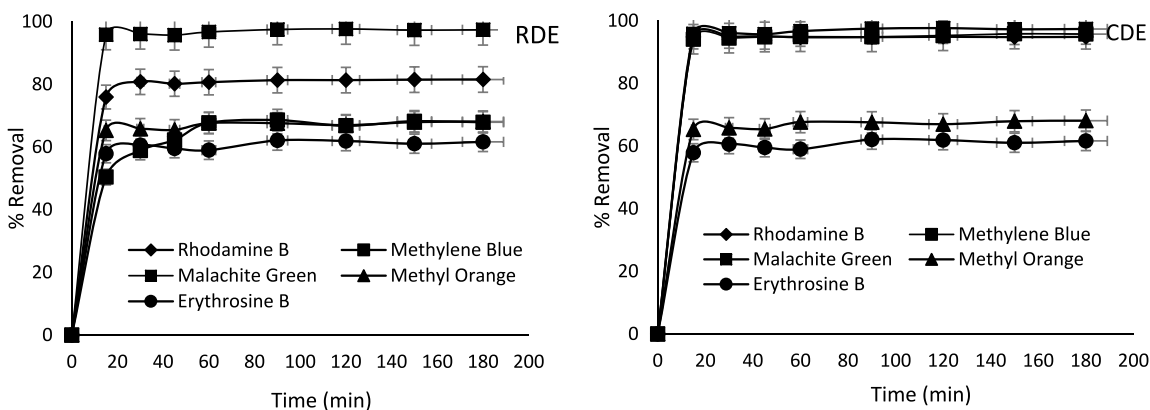
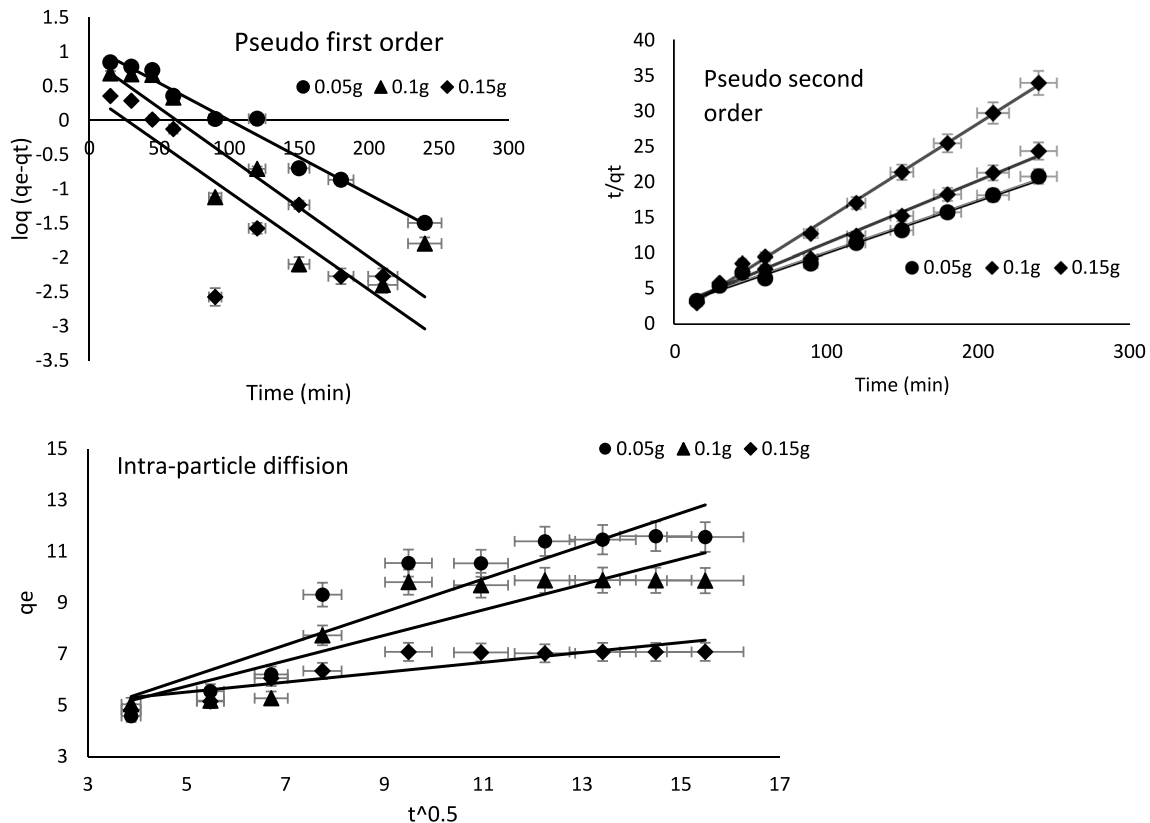


Fig. 12 Removal efficiency of RDE and CDE on selected dyes

Table 2 Kinetic model parameters for RDE and CDE

Mases	q_e (mg/g)	K_1 (min^{-1})	R^2	Exp q_e (mg/g)	K_2 (mg/g min^{-1})	R^2	K_p ($\text{mg/g min}^{0.5}$)	C	R^2
<i>CDE</i>									
0.05–1.15	0.78–7.45	0.003–0.021	0.30–0.92	7.39–26.32	0.006–0.034	0.99–1.00	0.06–0.82	6.44–16.18	0.44–0.66
<i>RDE</i>									
0.05–1.15	2.40–12.13	0.025–0.033	0.68–0.98	7.08–10.54	0.002–0.02	0.98–0.99	0.19–0.64	2.85–4.55	0.78–0.86

**Fig. 13** Kinetic model plots of RDE

details the steps that the CR dye takes to migrate from an aqueous solution to the surface of the sorbent. These stages are (1) boundary layer diffusion of CR dye molecules from aqueous solution to the surface of the sorbent, (ii) intra-particle diffusion of CR dye molecules, and (iii) sorption of CR dye molecules to the sorbent's active sites, which is the equilibrium stage (Rápó et al. 2020). The fact that the plot of q_e against $t^{0.5}$ is linear indicates that the rate-controlling phase involves intra-particle diffusion. However, the fact that the linear plot did not pass through the origin and the intercept value is smaller than 0 suggests that there are additional rate-controlling processes besides intra-particle diffusion. This implies that the sorption process involves both surface sorption and intra-particle diffusion, leading to a complicated sorption mechanism (Singh et al. 2020).

Sorption isotherms

Various linearized plots of isotherm models are shown in Figs. 15 and 16. Table 3 shows values for isotherm model parameters based on the slopes and intercepts of these plots. These findings demonstrate that the Langmuir isotherm model, which had the greatest R^2 values, provided the best fit for the sorption data. This is presuming that monolayer sorption took place on a flat, homogeneous sorbent surface. A separation factor, also known as a dimensionless constant, further supported the sorption process' adherence to the Langmuir model (R_L). The R_L values recorded were in the range of 0 and 1, which suggests that the sorption process is advantageous. Additionally, the sorption intensity (n) of the Freundlich model

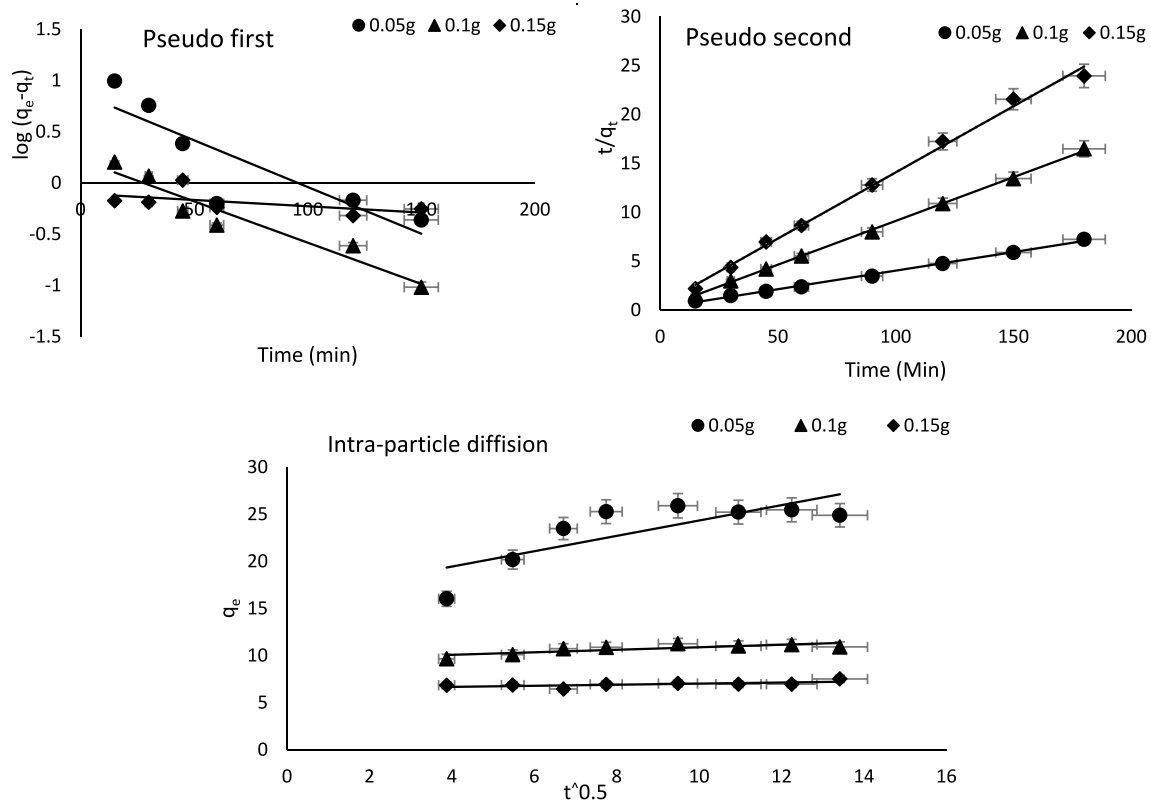


Fig. 14 Kinetic model plots of CDE

showed values greater than one, which is also a sign that the sorption process was favorable by the model.

According to the Temkin isotherm model, sorbate–sorbent interaction causes the heat of sorption of the sorbate's molecule to linearly decrease with sorbent layer coverage (Temkin and Pyzhev, 1940). The plots of q_e against $\ln C_e$ produced linear graphs, and according to the parameter values, K_T decreased for RDE but increased for CDE as temperature rose. Temkin's model, however, did not offer the greatest match for the sorption data and showed the lowest R^2 values when compared to other models. Comparable investigations using different plant-based sorbents on the adsorptive removal of CR dye from aqueous solution also demonstrated compliance to the Langmuir isotherm model. Table 4 presents the comparison of the maximum sorption capacity of these sorbents and others reported in literature for the sequestration of CR, although the sorption operating conditions were different. It is crucial to notice that CDE recorded higher CR removal in comparison to RDE. Studies by Yan et al. (2018) and Zhang et al. (2019) found that CA-modified sorbent had a greater sorption capacity than raw sorbent.

Thermodynamics of the sorption process

The linear graphs in Fig. 17 was obtained from the Van't Hoff plot of $\ln K_o$ against $(1/T)$. The values obtained for all the parameters are shown in Supplementary Table 1. The change in enthalpy (ΔH°) and entropy (ΔS°) was estimated from the slope and intercept of the graphs. At all operating temperatures, CR dye sorption onto both RDE and CDE produced negative ΔG° values, suggesting that the sorption processes were both spontaneous and possible. When CR dye molecules bind to the active sites, there is an increase in randomness at the sorbent–sorbate interface, as seen by the positive value of ΔS° obtained for both sorbents. Additionally, the positive value of ΔS° suggests that CR dye molecules are attracted to the sorbent favorably. However, sorption of CR dye unto RDE displayed negative ΔH° value, which infers exothermic sorption process, while that of CDE was endothermic because of the positive ΔH° value. Comparable observations have been reported in the literature for sorption of CR unto other raw and acid-modified sorbents (Rao and Rao 2016; Ojo et al. 2017; Lafi et al. 2019; Litefti et al. 2019).

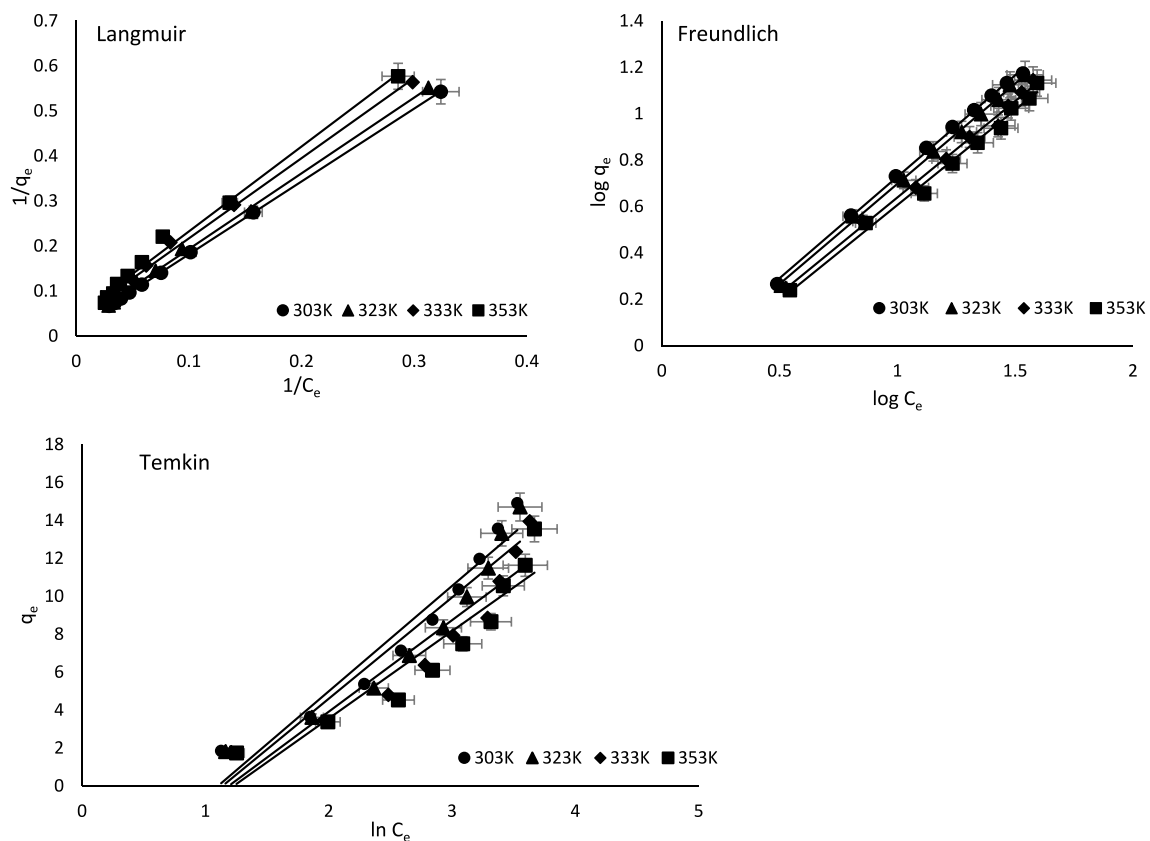


Fig. 15 Isotherm model plots of RDE

Adsorption mechanism

The sorbent's surface functional groups and the CR dye molecule are believed to have formed hydrogen bonds and electrostatic interactions that caused the sorbate and sorbent to bind together. For RDE and CDE, the point of zero charge was measured to be 6.2 and 2.8, respectively. This means that the $R-SO_3^-$ group in the CR dye molecule can be attracted to the surface of the sorbent in acidic media via electrostatic interaction. Additionally, at low pH levels, the functional groups of the sorbents such as OH, C=O and COOH can readily protonate and attract the negative ions on the sorbate. FTIR of CDE also shows that the functional groups which were previously available before sorption such as 2913 and 2845 cm^{-1} diminished afterward, indicating a bond between the dye and the group during adsorption.

Consequently, as pH rises, it is anticipated that the functional groups on the surface of the sorbent will fully ionize, leading to an electrostatic attraction between the CR and the surface of the sorbent. However, the functional groups tend to repel each other, resulting in a decreased sorption capacity of the sorbent (Lafi et al. 2019). Additionally, the development of hydrogen bonds as a secondary force of attraction in the sorption process is more probable (Ahmad and Kumar

2010). This is due to the sorbent and sorbate's surfaces having hydrogen and highly electronegative atoms like oxygen and nitrogen. Three interactions between the sorbent and dye molecule are likely, according to earlier research (i) hydrogen bonding between hydroxyl groups of sorbent and electronegative groups of CR dye, (ii) ionic interaction at pH value where surface charge is neutral and physisorption occurs and (iii) π -electron resonance (Zhang et al. 2019; Rapo et al. 2020).

Desorption research/regeneration

Figure 18 displays the data plots from the desorption experiment. Three desorbing agents were used in the desorption experiment: 0.1 M HCl, 0.1 M NaOH and deionized water. The 0.1 M NaOH solution, which recorded the highest desorption efficiency among the three investigated solvents, most efficiently regenerated the used sorbents. This shows that electrostatic interaction and hydrogen bonding dominate the sorption process (Ahmad and Kumar 2010; Lafi et al. 2019). The migration of CR dye molecules from the solid to liquid phase was influenced by the solvating strength, desorbing agent concentration and agitation rate (Momina et al. 2019).

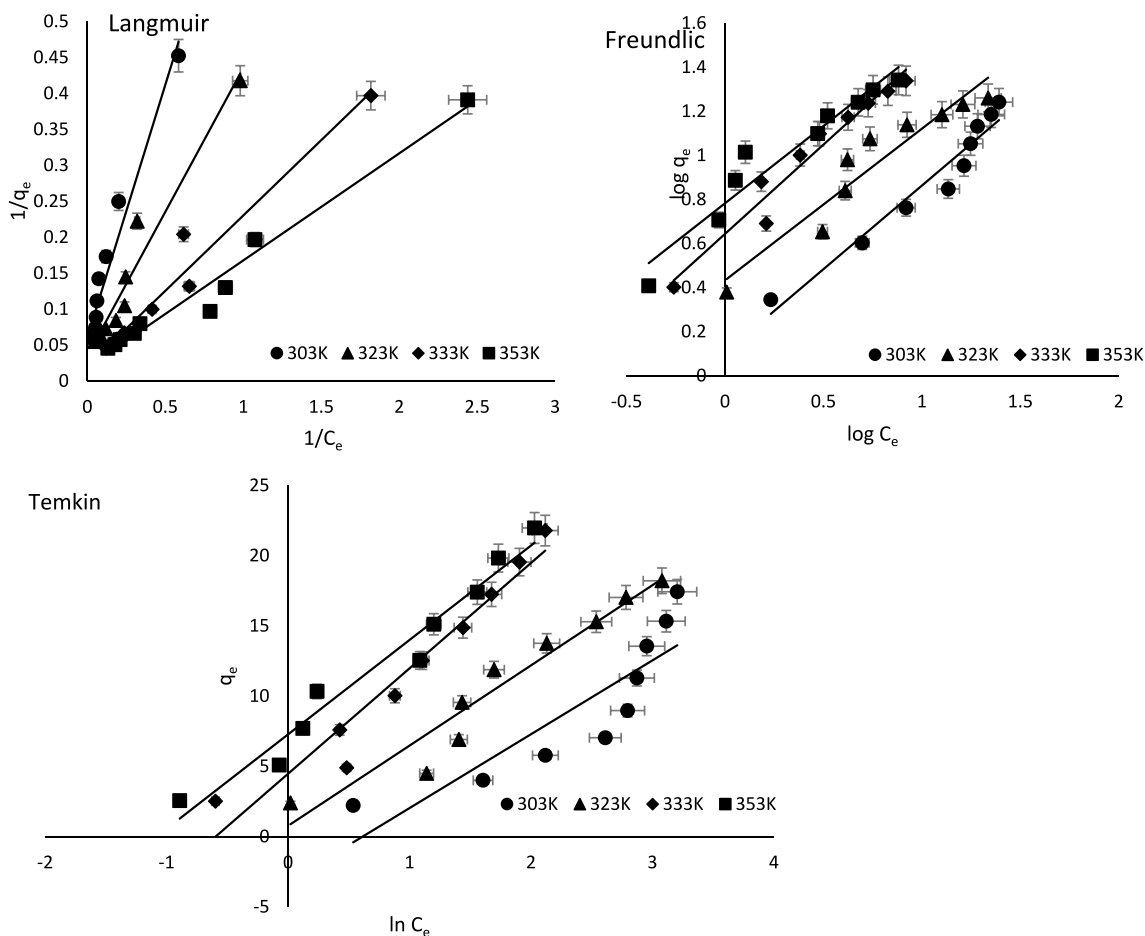


Fig. 16 Isotherm model plots of CDE

Table 3 Isotherm models parameters for adsorption of CR dye onto RDE and CDE

Temp (K)	Langmuir model				Freundlich model			Temkin model		
	q_{max} (mg/g)	K_L (L/mg)	R_L	R^2	K_F (L/mg)	N	R^2	K_T (L/g)	B (J/mol)	R^2
<i>CDE</i>										
303–353	16.48–53.19	0.098–0.126	0.081–0.114	0.947–0.974	1.27–6.06	1.23–1.45	0.907–0.956	0.54–2.95	5.26–7.50	0.762–0.964
<i>RDE</i>										
303–353	22.83–51.02	0.01–0.02	0.33–0.48	0.995–0.999	0.61–0.71	1.14–1.22	0.991–0.998	0.29–0.33	4.61–5.56	0.879–0.939

Additionally, five sequential cycles of repeated washing of sorbents with 0.1 M NaOH were used to conduct an experiment on regeneration and reuse. For the second and third cycles as shown in Fig. 18, sorbents were able to adsorb CR dye at a level that was comparable to the virgin (1st cycle) samples. Sorption efficiencies during the fourth and fifth cycles show a sharp drop.

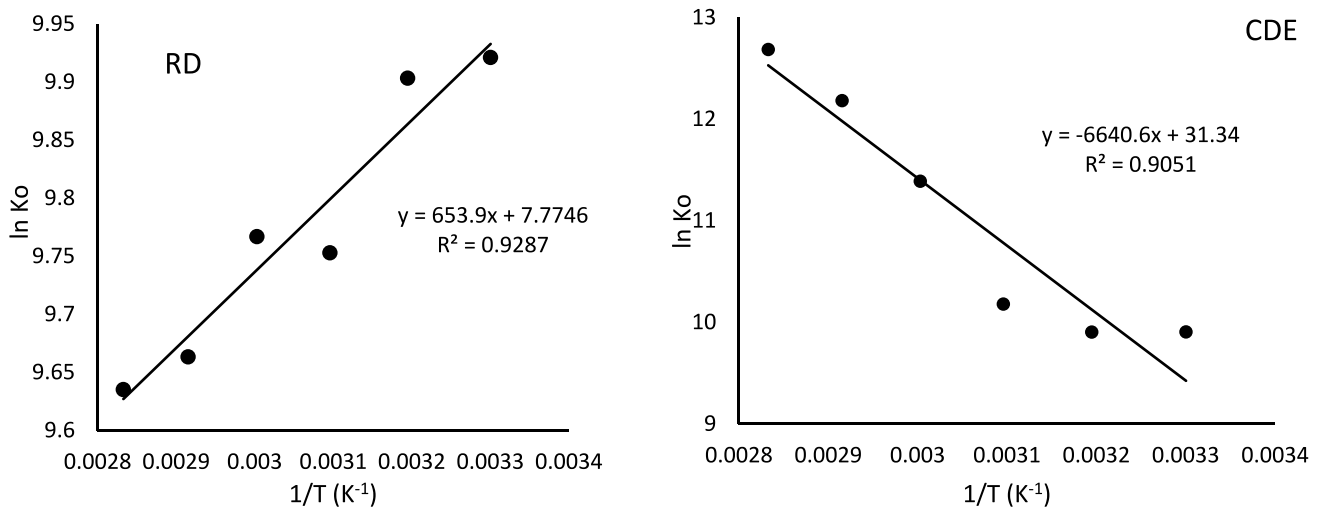
It may be difficult to recover 100% of the sorbent's mass from solution and the alkaline solution has changed the sorbents' surface structures, both of which contribute

to the fall in sorption effectiveness (Liu et al. 2018). As a result, sorption sites may be lost, damaged or blocked. Lafi et al. (2019) have documented a similar usage of NaOH as a successful desorbing solvent.

In conclusion, this study confirms that the novel sorbents may be recycled and re-utilized, making it a practical sorbent for removing hazardous dyes from aqueous solutions. The used sorbent can be properly disposed of in a regulated landfill that accepts hazardous waste.

Table 4 Maximum sorption capacity of CR dye onto various sorbents in literature

Plant-based sorbent	Maximum quantity sorbed (mg/g)	References
<i>CDE</i>	53.19	This study
<i>RDE</i>	51.03	This study
<i>Carpobrotus Edulis</i> Plant	7.86	Aziam et al. (2022)
Litchi seed powder	20.49	Edokpayi and Makete (2021)
Cuticle-removed cladodes (CRC) from <i>Cereus</i> spp.	27.02	Jeyavishnu and Alagesan (2020)
Cabbage waste powder	2.31	Wekoye et al. (2020)
Modified coffee waste	34.36	Wong et al. (2020)
Cuticle from <i>Cereus</i> spp.	52.63	Jeyavishnu and Alagesan (2020)
Pine bark	3.92	Litefti et al. (2019)
Modified <i>Luffa cylindrica</i> fiber	19.24	Pathania et al. (2017)
Phoenix <i>dactylifera</i> seeds	61.72	Pathania et al. (2016)
Pineapple stem	11.97	Chan and Ong (2016)

**Fig. 17** Van't Hoff plots of CR dye sorption onto RDE and CDE

Conclusion

DE is a locally available plant material in Vhembe District, Limpopo Province, South Africa. Raw DE (RDE) and citric acid-modified DE (CDE) were both studied for CR removal from aqueous solution via adsorption technique. FTIR spectra of RDE and CDE showed similar functional groups (O–H, CH– and C–O), while CDE displayed a shift to higher absorbance as well as the introduction of new functional groups such as 1589, 1621, 2913 and 2845 cm^{-1} . SEM clearly confirmed the modification of CDE with a larger surface area and a flaky structural surface when compared to RDE. Furthermore, EDS showed an increase in carbon atom percentage and decrease in oxygen compared to RDE which was linked to improved dye

removal from water. The BET surface area also revealed a higher surface area for CDE and RDE, thus implying a higher sorption capacity. The pzc of both adsorbents was in the acidic region which facilitated the attraction of anionic dyes via electrostatic attraction. CDE produced better removal than RDE with optimum experimental parameters of pH 2, 60 min contact time, adsorbent dosage of 1.5/L and high operating temperatures. Surface water samples were also used and the results showed better CR removal than deionized water. Consequently, CDE was also used for the removal of five additional dyes (cationic dyes and as anionic dyes) though the sequestration was higher for the anionic dyes. Regeneration was also possible with RDE and CDE adsorbing CR as effectively as the virgin adsorbent during the first 3 cycles, after which a decreased was observed in the fourth and fifth cycle. The Langmuir

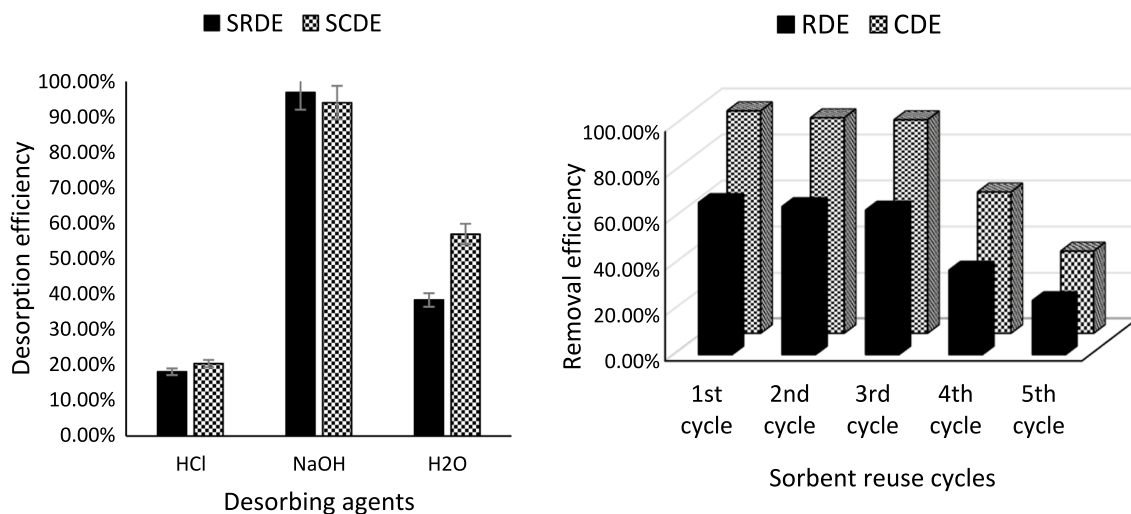


Fig. 18 Desorption of spent sorbents (left) and regeneration and reuse cycles of RDE and CDE (right)

model of monolayer sorption best described the sorption process with a maximum sorption capacity of 51.02 mg/g for RDE and 53.19 mg/g for CDE, respectively. The sorption process was spontaneous and endothermic for CDE but was exothermic for RDE.

Supplementary Information The online version contains supplementary material available at <https://doi.org/10.1007/s13201-024-02114-5>.

Author contributions All the authors contributed to the conception of the study and design. Mobolaji M. Jegede collected the materials and did the initial batch studies under the guidance of Prof. Joshua N. Edokpayi and Dr. Olatunde S. Durowoju. All the authors contributed to the methods of the study. Prof. Joshua N. Edokpayi provided the financial support of the study. Data analyses were performed by Dr. Olatunde S. Durowoju. All the authors wrote the first draft of the manuscript and agreed to the submission of the manuscript.

Funding This work was supported by the National Research Foundation of South Africa, (Grant number: (UID:127276) and University Capacity Development Grant (Grant number: R035) given to Prof JN Edokpayi.

Availability of data and materials The data used in this study are provided within the text of the manuscript. More information can be provided upon request from the corresponding author.

Declarations

Conflict of interest The authors declare no conflict of interest.

Ethical approval This study was reviewed by the Research Ethics Committee of the University of Venda with reference number: SES/21/HWR/10/0405.

Consent to participate Not applicable.

Consent to publish Not applicable.

Open Access This article is licensed under a Creative Commons Attribution 4.0 International License, which permits use, sharing,

adaptation, distribution and reproduction in any medium or format, as long as you give appropriate credit to the original author(s) and the source, provide a link to the Creative Commons licence, and indicate if changes were made. The images or other third party material in this article are included in the article's Creative Commons licence, unless indicated otherwise in a credit line to the material. If material is not included in the article's Creative Commons licence and your intended use is not permitted by statutory regulation or exceeds the permitted use, you will need to obtain permission directly from the copyright holder. To view a copy of this licence, visit <http://creativecommons.org/licenses/by/4.0/>.

References

- Ahmad R, Kumar R (2010) Adsorptive removal of congo red dye from aqueous solution using bael shell carbon. *Appl Surf Sci* 257:1628–1633
- Aziam R, Boukarma L, Abali M, Zerbet M, Sinan F, et al (2022) Equilibrium and Thermodynamic Studies for the Removal of Anionic Congo Red Dye by *Carpobrotus Edulis* Plant as Low-Cost Biomaterial. *J Material Sciences & Manufacturing Research. SRC/JMSMR-150*. [https://doi.org/10.47363/JMSMR/2022\(3\)138](https://doi.org/10.47363/JMSMR/2022(3)138)
- Barrett EP, Joyner LG, Halenda PP (1951) The determination of pore volume and area distributions in porous substances. I. Computations from nitrogen isotherms. *J Am Chem Soc* 73:373–380
- Bello OS, Auta M, Ayodele OB (2013) Ackee apple (*Blighia sapida*) seeds: a novel adsorbent for the removal of Congo red dye from aqueous solutions. *Chem Ecol* 29(1):58–71
- Bello OS, Alabi EO, Adegoke KA, Adegboye SA, Inyinbor AA, Dada AO (2020) Rhodamine B dye sequestration using *Gmelina aborea* leaf powder. *Heliyon*
- Berradi M, Hsissou R, Khudhair M, Assouag M, Cherkaoui O, El Bachiri A, El Harfi A (2019) Textile finishing dyes and their impact on aquatic environs. *Heliyon*, pp 1–11
- Brunauer S, Emmett PH, Teller E (1938) Adsorption of gases in multimolecular layers. *J Am Chem Soc* 60(2):309–319
- Bwatanglang IB, Magili ST, Mohammad F, Al-Lohedan HA, Soleiman AA (2023) Biomass-based silica/calcium carbonate nanocomposites for the adsorptive removal of *Escherichia coli* from aqueous suspensions. *Separations* 10(3):1–17

- Corda NC, Kini MS (2018) Review on adsorption of cationic dyes using activated carbon. MATEC Web Conf 144(02022):1–16
- Chan SL, Ong ST (2016) Equilibrium, kinetic and thermodynamic studies of a few potential biosorbent for the removal of Basic Blue 3 and Congo red dyes: pineapple (*Ananas comosus*) plant stem. J Taiwan Inst Chem Eng 61:306–315
- Edokpayi JN, Makete E (2021) Removal of Congo red dye from aqueous media using Litchi seeds powder: Equilibrium, kinetics and thermodynamics. Phys Chem Earth 123(7):1–9
- Edokpayi JN, Alayande SO, Adetoro A, Odiyo JO (2020) The equilibrium, kinetics, and thermodynamics studies of the sorption of methylene blue from aqueous solution using pulverized raw macademia nut shells. J Anal Methods Chem, pp 1–10
- Edokpayi JN, Ndlovu SS, Odiyo OJ (2019) Characterization of pulverized Marula seed husk and its potential for the sequestration of methylene blue from aqueous solution. BMC Chem 13(10):1–14
- Edokpayi JN, Odiyo JO, Msagati TAM, Popoola EO (2015) A novel approach for the removal of lead (II) Ion from wastewater using mucilaginous leaves of *Diceriocaryum eriocarpum* plant. Sustainability 7:14026–14041
- Farias RS, Buarque HL, Cruz MB, Cardoso LMF, Gondim TA, Paulo VR (2017) Adsorption of congo red dye from aqueous solution onto amino-functionalized silica gel. Engenharia Sanitária e Ambiental 23(6):1053–1060
- Felista MM, Wanyonyi WC, Gilbert O (2020) Adsorption of anionic dye (Reactive Black 5) using macadamia seed husks: kinetics and equilibrium studies. Sci African, pp 1–10
- Freundlich HMF (1906) Over the adsorption in solution. Z Phys Chemie (leipzig) 57:385–470
- Hambisa AA, Regasa MB, Ejigu HG, Senbeto CB (2023) Adsorption studies of methyl orange dye removal from aqueous solution using anchote peel-based agricultural waste adsorbent. Appl Water Sci 13 (24):1–11
- Harja M, Buema G, Bucur D (2020) Recent advances in removal of Congo Red dye by adsorption using an industrial waste. Sci Rep 2022 12:6087. <https://doi.org/10.1038/s41598-022-10093-3>
- Ho YS, McKay G (1998) Kinetic model for lead(II) sorption on to peat. Adsorpt Sci Technol 16:243–255. <https://doi.org/10.1177/026361749801600401>
- Inyinbor AA, Adekola FA, Olatunji GA (2015) Adsorption of rhodamine B dye from aqueous solution on *Irvingia gabonensis* Biomass: kinetics and Thermodynamics Studies. S Afr J Chem 68:115–125
- Javid N, Honarmandrad Z, Malakootian M (2020) Ciprofloxacin removal from aqueous solutions by ozonation with calcium peroxide. Desalin Water Treat 174:178–185
- Jegade MM, Durowoju OS, Edokpayi JN (2021) Sequestration of hazardous dyes from aqueous solution using raw and modified agricultural waste. Adsorp Sci Technol, pp 1–21
- Jeyavishnu K, Alagesan V (2020) *Cereus* sp. as potential biosorbent for removal of Congo red from aqueous solution: isotherm and kinetic investigations. Environ Monitor Assess 192: 243
- Khan MI, Akhtar S, Zafar S, Shaheen A, Khan MA, Luque R, Rehman A (2015) Removal of congo red from aqueous solution by anion exchange membrane (EBTAC): adsorption kinetics and themodynamics. Materials 8:4147–4161
- Kong S, Huang X, Li K, Song X (2019) Adsorption/desorption isotherms of CH₄ and C₂H₆ on typical shale samples. Fuel 255:1–8
- Lafi R, Montasser I, Hafiane A (2019) Adsorption of congo red dye from aqueous solutions by prepared activated carbon with oxygen-containing functional groups and its regeneration. Adsorpt Sci Technol 37(1–2):160–181
- Lagergren SK (1898) About the theory of so-called adsorption of soluble substances. Kung Svenska Veenskapsakad Handlingari 24:1–39
- Langmuir I (1916) The constitution and fundamental properties of solids and liquids. J Am Chem Soc 38(11):2221–2295
- Lin D, Wu F, Hu Y, Zhang T, Liu C, Hu Q, Hu Y, Xue Z, Han H, Ko T (2020) Adsorption of dye by waste black tea powder: parameters, kinetic, equilibrium, and thermodynamic studies. Hindawi J Chem, pp 1–13
- Litefti K, Freire MS, Stitou M, González-Álvarez J (2019) Adsorption of an anionic dye (Congo red) from aqueous solutions by pine bark. Nature Sci Rep 9:1–13
- Liu L, Fan S, Li Y (2018) Removal behavior of methylene blue from aqueous solution by tea waste: kinetics, isotherms, and mechanism. Int J Environ Res Public Health 15(7):1321–1337
- Lippens B, De Boer J (1965) Studies on pore systems in catalysts: V. The t method. J Catal 4:319–323
- Mannzhi MP, Edokpayi JN (2023) Fluoride sorption using Al and Mg modified dicerocaryum eriocarpum leaves mucilage. Environ Technol Innov 30:103075. <https://doi.org/10.1016/j.eti.2023.103075>
- Manzoor K, Batool M, Naz F, Nazar MF, Hameed BH, Zafar MN (2022) A comprehensive review on application of plant-based bio-adsorbents for Congo red removal. Biomass Convers Biorefinery. <https://doi.org/10.1007/s13399-022-02741-5>
- Mohebal S, Bastani D, Shayesteh H (2019) Equilibrium, kinetic and thermodynamic studies of a low-cost biosorbent for the removal of Congo red dye: acid and CTAB-acid modified celery (*Apium graveolens*). J Mol Struct 1176:181–193
- Momina, Rafatullah M, Ismail S, Ahmad A (2019) Optimization study for the desorption of methylene blue dye from clay based adsorbent coating. Water 11 (1304):1–13
- Odiyo JO, Bassej OJ, Ochieng A, Chimuka L (2017) Coagulation efficiency of dicerocaryum eriocarpum (DE) plant. Water SA 43(1):1–6
- Ojo TA, Ojedokun AT, Bello OS (2017) Functionalization of powdered walnut shell with orthophosphoric acid for Congo red dye removal. Particulate Sci Technol, pp 1–13
- Olakunle MO, Inyinbor AA, Dada AO, Bello OS (2017) Combating dye pollution using cocoa pod husks: a sustainable approach. Int J Sustain Eng, pp 1–13
- Ologundudu TO, Odiyo JO, Ekosse GE (2016) Fluoride sorption efficiency of vermiculite functionalised with cationic surfactant: isotherm and kinetics. Appl Sci 6(277):1–15
- Oyekanmi AA, Ahmad A, Hossain K, Rafatullah M (2019) Adsorption of Rhodamine B dye from aqueous solution onto acid treated banana peel: response surface methodology, kinetics, and isotherm studies. PLoS ONE 14(5):1–20
- Pathania D, Sharma A, Siddiqi ZM (2016) Removal of congo red dye from aqueous system using Phoenix dactylifera seeds. J Mol Liq 219:359–367
- Pathania D, Sharma A, Sethi V (2017) Microwave induced graft copolymerization of binary monomers onto luffacylindrica fiber: removal of Congo red, Procedia Engineering 200:408–415. <https://doi.org/10.1016/j.proeng.2017.07.057>
- Rao TM, Rao VVB (2016) Biosorption of Congo Red from aqueous solution by crab shell residue: a comprehensive study. Springerplus 5(537):1–14
- Rápó E, Aradi LE, Szabó A, Posta K, Szép R, Tonk S (2020) Adsorption of Remazol brilliant violet-5R textile dye from aqueous solutions by using eggshell waste biosorbent. Sci Rep, pp 1–12
- Ren Y, Cui C, Wang P (2018) Pomelo peel modified with citrate as a sustainable adsorbent for removal of methylene blue from aqueous solution. Molecule 23:1–13
- Sarkar S, Banerjee A, Halder U, Biswas R, Bandopadhyay R (2017) Degradation of synthetic azo dyes of textile industry: a sustainable approach using microbial enzymes. Water Conserv Sci Eng 2:121–131

- Sen TK (2023) Adsorptive removal of dye (methylene blue) organic pollutant from water by pine tree leaf biomass adsorbent. *Processes* 11(7):1877
- Sharma S, Tiwari DP (2016) Model-fitting approach for methylene blue dye adsorption on Camelina and Sapindus seeds-derived adsorbents. *Adsorpt Sci Technol* 34(9–10):565–580
- Sing KSW, Everett DH, Haul RAW, Moscou L, Pierotti RA, Rouquerol J, Siemieniewska T (1985) Reporting physisorption data for gas/solid systems with special reference to the determination of surface area and porosity. *Pure Appl Chem* 57(4):603–619
- Singh R, Singh TS, Odiyo JO, Smith JA, Edokpayi JN (2020) Evaluation of methylene blue sorption onto low-cost biosorbents: equilibrium, kinetics, and thermodynamics. *J Chem*, pp 1–12
- Tarmizi T, Risfidian M, Rohendi D, Lesbani A (2017) Kinetic and thermodynamic adsorption studies of Congo red on bentonite. In: AIP conference proceedings, Yogyakarta: AIP Publishing, vol. 1823, pp 020028-1–020028-8
- Temkin M, Pyzhev V (1940) Kinetics of ammonia synthesis on promoted iron catalysts. *Acta Physicochimica URSS* 12(3):217–222
- Toor MK (2010) Enhancing adsorption capacity of Bentonite for dye removal: physicochemical modification and characterization in Department of Chemical Engineering. University of Adelaide, p 209
- Van't Hoff JH (1884) Studies in dynamic chemistry. <https://www.nobelprize.org/prizes/chemistry/1901/hoff/biographical/>
- Webber WJ, Morris JC (1963) Kinetics of adsorption on carbon from solution. *J Sanitary Eng Div ASCE* 89:31–60
- Wekoye JN, Wanyonyi WC, Wangila PT, Tonui MK (2020) Kinetic and equilibrium studies of Congo red dye adsorption on cabbage waste powder. *Environ Chem Ecotoxicol* 2:24–31
- Wong S, Abd Ghafar N, Ngadi N, Razmi FA, Inuwa IM, Mat R, Amin NAS (2020) Effective removal of anionic textile dyes using adsorbent synthesized from coffee waste. *Sci Rep*, pp 1–10
- Yagub MT, Sen TK, Afroze S, Ang HM (2014) Dye and its removal from aqueous solution by adsorption: a review. *Adv Coll Interface Sci* 209:172–184
- Yan J, Lan G, Qiu H, Chen C, Liu Y, Du G (2018) Adsorption of heavy metals and methylene blue from aqueous solution with citric acid modified peach stone. *Sep Sci Technol* 11:1678–1688
- Zaharia C, Suteu D (2009) Optimization study of Orange 16 dye sorption onto sawdust wastes. *Bull Inst Politechnic, Iasi, series: Chemistry and Chemical engineering, tom LV (LIX), f. vol 4*, pp 103–113
- Zhang H, Zhou J, Muhammad Y, Tang R, Liu K, Zhu Y, Tong Z (2019) Citric acid modified bentonite for Congo red adsorption. *Front Mater* 6(5):1–11
- Zhou Y, Ge L, Fan N (2018) Adsorption of Congo red from aqueous solution onto shrimp shell powder. *Adsorpt Sci Technol* 36(5–6):1310–1330

Publisher's Note Springer Nature remains neutral with regard to jurisdictional claims in published maps and institutional affiliations.